



*J. Serb. Chem. Soc.* 87 (7–8) 867–877 (2022)  
JSCS–5563

## Supercapacitive properties of the alkali metal hydroxides-activated carbons obtained from sucrose<sup>•</sup>

MILICA G. KOŠEVIĆ<sup>1\*#</sup>, SANJA S. KRSTIĆ<sup>2</sup>, VLADIMIR V. PANIĆ<sup>1,3,4#</sup>  
and BRANISLAV Ž. NIKOLIĆ<sup>5#</sup>

<sup>1</sup>Institute of Chemistry, Technology and Metallurgy, National Institute of the Republic of Serbia, University of Belgrade, Belgrade, Serbia, <sup>2</sup>University of Belgrade, Vinča Institute of Nuclear Sciences, Belgrade, Serbia, <sup>3</sup>Centre of Excellence in Environmental Chemistry and Engineering – ICTM, University of Belgrade, Belgrade, Serbia, <sup>4</sup>State University of Novi Pazar, Department of Natural and Mathematical Sciences, Novi Pazar, Serbia and <sup>5</sup>Faculty of Technology and Metallurgy, University of Belgrade, Belgrade, Serbia

(Received 30 June, revised and accepted 18 July 2022)

**Abstract:** The influence of different hydroxides, applied to activate carbon black, on the electrochemical properties of activated carbon was investigated. The carbon material was prepared by hydrothermal treatment of sucrose and afterwards thermally activated using KOH, NaOH and LiOH. The electrochemical properties of the obtained samples were examined by cyclic voltammetry and electrochemical impedance spectroscopy and correlated to their physico-chemical properties. All samples showed characteristic capacitor-like behaviour. The highest specific capacitance was obtained for the KOH-treated sample, while the increase in capacitance follows the sequence of the growth of ionic radius of a metal from an alkali which is used for activation. It was found that the dependence on the type of hydroxide is due to differences in the radii of a metal. The alkalis of larger radii of metal generated make pores wider and consequently the structure of a porous layer become more accessible to the charge transfer of capacitive response.

**Keywords:** sucrose-derived carbons; alkali-treated carbon materials; sugar-derived carbons; electrochemical capacitance distribution.

\* Corresponding author. E-mail: milica.kosevic@ihm.bg.ac.rs

# Serbian Chemical Society member.

• This paper is dedicated to our distinguished colleagues, Radoslav Atanasoski and Radoslav Adžić, to honour their 80<sup>th</sup> birthday anniversaries (born in January and February 1942, respectively). Both of them gave outstanding contribution to the contemporary electrochemistry, particularly to electrocatalysis and fuel cell development. During decades, being outstanding scientists, they were our coworkers and teachers, but also exceptionally good friends. We wish to both of these great men all the best for many years to come.

<https://doi.org/10.2298/JSC220730059K>

## INTRODUCTION

Emerging advances in modern electronics have been given rise to increased necessities for highly efficient energy storage systems. As one of the most popular type of electrochemical energy storage systems, supercapacitors recently gained the highest attention owing to the following characteristics: high power density, structure-dependent charge/discharge rate, energy density, environmental friendliness, rentability, long cycle life, *etc.*<sup>1,2</sup> Their superior capacitive properties originate not only from the charge stored in an electrochemical double layer, but also from the fast and highly reversible Faradaic reactions occurring at the electrode/electrolyte interface, which results in the so-called pseudocapacitance.<sup>3,4</sup> These unique performances are obtained from different redox-active and porous electrode materials, especially noble metal oxides,<sup>5</sup> but also from carbon-based materials,<sup>2,6–9</sup> including activated carbons,<sup>10–14</sup> graphene,<sup>4,15–17</sup> carbon nanogels<sup>18</sup> and carbon nanotubes.<sup>19,20</sup> Carbon-based materials are among the most popular for supercapacitor application. They possess the required properties such as high surface area, low specific volume, controllable pore size, good electrical and thermal conductivity, acceptable chemical stability. The most important feature are low synthesis costs, since carbon-based materials can be obtained from a variety of cheap and waste precursor materials.<sup>21,22</sup> Environmentally friendly and economically acceptable precursors are definitely the main advantage of the carbon-based materials of excellent capacitive properties. Numerous studies of waste biomass-derived active carbons demonstrate their high specific surface areas, as well as specific capacitance values. K<sub>2</sub>CO<sub>3</sub>-activated waste tea-derived carbon can deliver specific capacitance of 123 F g<sup>-1</sup>.<sup>10</sup> KOH-activated calyx biowaste-derived carbons possesses the specific surface area of 798 m<sup>2</sup> g<sup>-1</sup> able to release the specific capacitance of 223 F g<sup>-1</sup> at 1 A g<sup>-1</sup> discharge current.<sup>11</sup> NaOH-activated carbon materials derived from heavy bio-oils give specific surface area as high as 2826 m<sup>2</sup> g<sup>-1</sup> and the specific capacitances of 417 F/g at 0.5 A g<sup>-1</sup> and 334 F g<sup>-1</sup> at 20 A g<sup>-1</sup>.<sup>12</sup> Even self-activated wood-derived carbon material delivers specific capacitance of 143.6 F g<sup>-1</sup> at 1 A g<sup>-1</sup> with surface area of 1145 m<sup>2</sup> g<sup>-1</sup>.<sup>13</sup> Charging capability and energy-delivering efficiency in supercapacitor systems request materials with high surface area and pores that fit to the relief of ionic transport throughout. The pore size distribution and its variability are controllable characteristics of the active carbon materials and they depend on different factors. Set of parameters in synthesis and corresponding approach involves the definition of synthesis precursor used and the type of activation method applied subsequently.

The activation method of carbon materials can be chemical or physical. Cai *et al.*<sup>23</sup> investigated the influence of the synthesis and activation conditions on the properties of the KOH-activated carbon. Specific surface area and capacitance of the carbon obtained from the glucose, another common and cheap pre-

cursor, significantly varied depending on the activation conditions, *i.e.*, synthesis temperature, sample/activation agent ratio, concentration of the precursor solutions, *etc.* Besides the mentioned synthesis conditions, activation processes are intrinsically governed by the type of activation agent that finally defines the porosity of the active product. Alkalies are widely used agents for chemical activation of carbon materials in the processes where the carbonization of organic precursors and activation process take place simultaneously.<sup>11,12,23,24</sup> These simultaneous processes significantly improve the structure and consequently capacitive properties. For example, the specific capacitance of the NaOH surface-activated commercial carbon cloth arose to  $42.2 \text{ F g}^{-1}$ , which is almost two orders of magnitude higher than the capacitance of the un-activated sample.<sup>24</sup> Beside alkalies, there are different chemical agents used for carbon activation, such as  $\text{K}_2\text{CO}_3$ ,<sup>10</sup>  $\text{H}_3\text{PO}_4$ <sup>10,25</sup> and  $\text{ZnCl}_2$ .<sup>26</sup>

This research involves the influence of the different alkali activation agents on the morphology and consequently the electrochemical properties of the activated carbon materials obtained from sucrose. Considering the aforementioned desired assets of the precursors, sucrose was chosen as a cheap, nontoxic and easily accessible precursor material. The carbon-containing material, which was obtained by hydrothermal method from sucrose, did not possess any remarkable capacitive properties. Hence, the experiment was further performed by chemical activation procedure employing several alkalies, KOH, NaOH and LiOH, in order to find the best capacitive outputs in a term of specific surface area, micro-porous morphology and finally the correlation between capacitive and physico-chemical properties, induced by the activation process.

## EXPERIMENTAL

### *Material synthesis*

Synthesis of the activated carbon materials was performed in two steps, as described in our previous work.<sup>27</sup> The first step is the hydrothermal treatment of the sucrose in order to obtain carbon-containing material, while in the second step carbonaceous materials were activated using hydroxides.

The required amount of sucrose was dissolved in the deionised water. The obtained  $1.0 \text{ mol dm}^{-3}$  solution was placed in an autoclave with polytetrafluoroethylene chamber and kept in an oven under autogenous pressure at  $240 \text{ }^\circ\text{C}$  for 24 h. The activation was performed afterwards by chemical treatment of the obtained sample with KOH, NaOH or LiOH. Activation of the samples was completed in an atmosphere of nitrogen, since the presence of oxygen would result in complete pyrolysis and generation of  $\text{CO}_2$ , which affects porosity development as well.<sup>28</sup> After the physical mixing of dried selected carbon-containing precursors and a hydroxide in solid state at room temperature in a mass ratio of 1:3, the solid mixtures were thermally treated in a horizontal tube furnace (Protherm Furnaces, model PTF 16/38/250, Turkey) at  $750 \text{ }^\circ\text{C}$ , under  $200 \text{ cm}^3 \text{ min}^{-1}$  of nitrogen flow and the heating rate of  $5 \text{ }^\circ\text{C min}^{-1}$ , with the retention time of 1 h. After carbonization and activation, the samples were washed with distilled water till the neutral pH value of effluent.

### Electrochemical measurements

Basic electrochemical characteristics of the synthesized samples were investigated using cyclic voltammetry (CV) technique. Depending on the CV response and its stability stages, some of the samples were afterwards subjected to the electrochemical impedance spectroscopy (EIS) to further investigate their capacitive features. All measurements were performed in 0.1 M H<sub>2</sub>SO<sub>4</sub> solution at ambient temperature. Cyclic voltammetry was done at the sweep rate of 50 mV s<sup>-1</sup>. The EIS was recorded in a single sine mode at open circuit potential, with a sinusoidal voltage of 10 mV-amplitude (root mean square).

Electrochemical measurements were recorded in a three-electrode cell with Ag/AgCl reference electrode and platinum plate as a counter electrode on potentiostat/galvanostat Bio-Logic SP200 (Bio-Logic SAS, Grenoble, France). All potentials are referred to Ag/AgCl scale. The working electrode was prepared by pipetting the 0.020 ml of the sample suspension onto a glassy carbon disk (GC, 0.196 cm<sup>2</sup>) electrode and dried at room temperature. Sample suspension consisted of 3 mg of alkali-treated carbon and 1 ml H<sub>2</sub>O and was ultrasonically treated (40 kHz, 70 W) for 1 h before application. To ensure the adhesion of the dry layer, it was covered by the nafion from appropriate solution (1:100 volume ratio of 10 mass % nafion solution in isopropanol/water and water).

Considering that registered EIS data were of capacitive-like shape, they were fitted into the transmission line equivalent electrical circuit (TLEEC) of time distributed constants using ZView (v. 3.2b, Scribner Associates Inc., Southern Pines, NC, USA). TLEEC consisted of resistors and capacitors in a notation  $R_{\Omega}(C_0(R_{p,1}(C_1(R_{p,2}(\dots(R_{p,n}C_n))))))$ , where  $C_n$  correlates to the capacitance available behind  $\sum_{i=1}^n R_{p,i}$  resistances;  $R_{\Omega}$  correlates to electrolyte ohmic resistance.

## RESULTS AND DISCUSSION

Characteristic cyclic voltammograms (CVs) of the as synthesized and alkali-treated samples are shown in Fig. 1.

All registered CV curves are of typical capacitor-like shape for carbon-based materials.<sup>29</sup> The CV currents of the untreated sample (Fig. 1b) are significantly lower in comparison to those registered for alkali-treated samples (Fig. 1a), which demonstrates excellent activation efficiency. Weakly pronounced anodic peaks around 0.50 (for S) and 0.25 V (for activated samples) appear to be redox ones, since cathodic counterparts are registered during discharging. The LiOH-treated sample shows more than five-fold increase in CV currents with respect to the untreated sample. On the other hand, this increase is more than two orders of magnitude for the KOH- and NaOH-treated samples. The treatment causes a development of a redox transition around 0.25 V, quite close to the typical position of quinonic surface redox response.<sup>30</sup> Fig. 1 clearly shows that the improvements of capacitive properties by alkali treatment are more pronounced for alkalies containing an alkali metal of larger ionic radius. This indicates that the surface states of carbon particles are different if treated by different alkalies, which produces significant varieties in capacitive properties.

The investigation of CV response stability showed that the alkali-treated samples required from several tens up to 200 cycles, depending on alkali used, to

reach the highest CV currents. The corresponding changes in capacitance<sup>31</sup> with cycling are shown in Fig. 2 for alkali-treated samples. The CV responses of the highest currents for KOH and LiOH treated samples were found to be unstable, since the currents gradually decreased upon subsequent cycling. This feature of decreasing CV currents was also alkali-dependent, varying from few tens for LiOH-treated sample to more than 100 cycles in a case of the S-KOH sample, for the currents to relax to the values of initial CV response. S-NaOH sample showed quite stable response upon the continuous increase in CV currents.

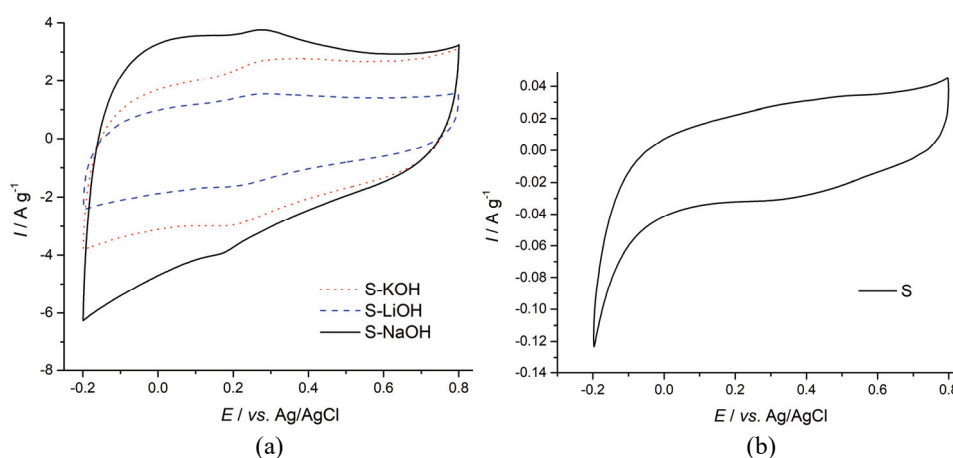


Fig. 1. Cyclic voltammograms of alkali-treated (a) and as-synthesized (b) carbons. Electrolyte: 0.1 M H<sub>2</sub>SO<sub>4</sub>,  $\nu = 50 \text{ mV s}^{-1}$ .

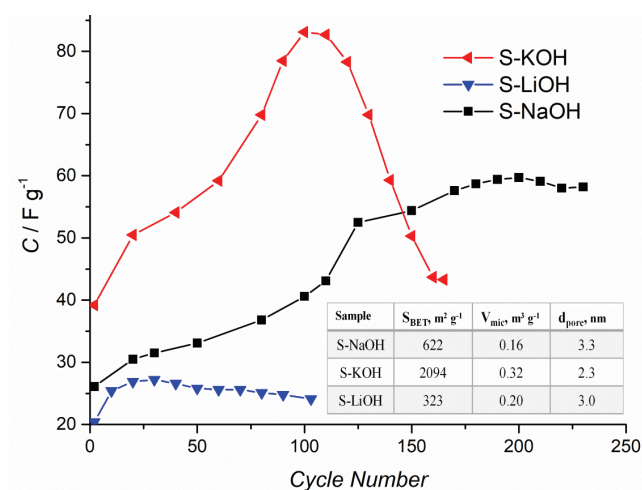


Fig. 2. Capacitance of alkali-treated samples during CV measurements. Electrolyte: 0.1 M H<sub>2</sub>SO<sub>4</sub>,  $\nu = 50 \text{ mV s}^{-1}$ . Inset:<sup>27</sup> morphological properties of activated carbons (S-XOH): specific surface areas ( $S_{\text{BET}}$ ), micropore volume ( $V_{\text{mic}}$ ) and average pore width ( $d_{\text{pore}}$ ).

The cycling initially produces the three-fold increase in capacitance upon 100 cycles for S-KOH sample. The highest specific capacitance registered in this most active charging/discharging cycle is around  $85 \text{ F g}^{-1}$ . However, this curing by cycling does not last, since subsequent cycling has an opposite effect – the capacitance is decreased to the initial values in next 65 cycles. In contrast to this unsteady capacitive behaviour, S-NaOH sample showed lower but stable capacitive response. Its capacitance steadily increases up to  $\sim 170$  cycle. Once reached, the maximum specific capacitance of  $60 \text{ F g}^{-1}$  was preserved in the following 50 cycles. Stabilizing influence of NaOH was proved also in other systems requiring modification of solid–liquid interface for coating deposition onto electrified surface.<sup>32,33</sup> Finally, the capacitance of LiOH-treated sample reached comparatively stable, but the lowest capacitance values of about  $25 \text{ F g}^{-1}$  during 100 cycles.

The changes from Fig. 2 could be caused by characteristic changes in the layer structures of KOH- and NaOH-treated samples induced by alkalis, and can be related to the samples' morphology parameters from the table shown as the inset of Fig. 2.<sup>27</sup> The values of maximum acquired specific capacitance are in an accordance with the samples' BET surface area. S-KOH exhibited the highest specific capacitance and this sample also possesses the highest specific area as well as the highest volume of micropores. In opposite to these highest values stands S-LiOH sample that exhibited both the lowest specific capacitance and specific area/volume of micropores. However, although samples' BET specific areas are in accordance with their maximum registered specific capacitances, this relation isn't proportional. Namely, the S-KOH surface is about 3.4 and 6.5 times larger than the surfaces of S-NaOH and S-LiOH samples, respectively, while the S-KOH maximum capacitance is only 1.4 and 3.3 times higher than those obtained for the S-NaOH and the S-LiOH, respectively. Moreover, the stable S-KOH specific capacitance is even lower than that of the S-NaOH, suggesting that capacitance isn't controlled solely by the BET surface area. According to the literature,<sup>29,34</sup> higher BET surface usually indicates higher capacitance. However, other parameters, like mesoporous surface and pore diameter, have also an effect on the capacitive behaviour. Although micropores (with pore diameter,  $d_p < 2 \text{ nm}$ ) should have an essential role in the capacitance, acting as a source of adsorption sites, their small dimension could hinder the ion access to nanoporous structure. Hence, the presence of the mesoporous microporous surface ( $d_p$  in the range 2–50 nm) is of essential importance for ion accessibility.<sup>35</sup>

Since CV findings revealed more stable capacitive nature of the NaOH and LiOH-treated samples in comparison to the S-KOH, the S-NaOH and S-LiOH samples were further investigated by EIS measurements. The registered and fitting EIS data of these samples are presented in a capacitive complex plane in Fig. 3.

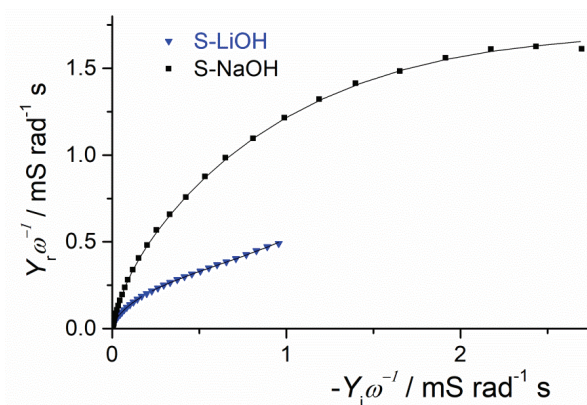


Fig. 3. Registered (symbols) and fitting (lines) EIS data of the S-LiOH and S-KOH samples.

Both samples showed capacitive loops, indicating their capacitive-like behaviour.

The S-NaOH related loop is considerably larger in comparison to the S-LiOH, suggesting its higher capacitance. This is in accordance with the capacitive values obtained from CV results (Fig. 1), where the S-NaOH sample also showed superior capacitive properties.

The differences in the samples' structure, reflected in the impedance characteristics (Fig. 3), are presented in Fig. 4 as the distributions of the pore resistance and the capacitance through a layer of the samples. The data were obtained by fitting the experimental EIS data to an appropriate TLEEC (as explained in Experimental; additional data are given in Supplementary material to this paper).

S-LiOH sample required higher number of the branches (higher  $n$ ) in comparison to the S-NaOH sample, *i.e.*, 5 compared to 2. TLEEC, described in Experimental, required the parallel resistor and capacitor elements in series to TLEEC. This RC circuit can be assigned to the nafion layer at the sample surface, since the capacitance values are at least one order of the magnitude lower in comparison to the capacitances in each individual of TLEEC. On the other hand,  $R$  values are comparable to those in the branches. Hence, the initial increase in capacitances observed in the Fig. 2 can be attributed to the resistance decrease due to continuous wetting of the nafion layer. As shown in Fig. 2, the S-NaOH sample reached highest capacitance considerably faster. This is in accordance with mentioned  $R$  values ascribed to the nafion layer. Namely, the resistance of the nafion layer on the top of the S-NaOH sample was considerably higher than that registered for S-LiOH, 62  $\Omega$ , in contrast to 16  $\Omega$ . It follows that the electrolyte needs longer time to overcome higher resistance of the nafion layer in order to get the full access to the sample's surface. The unexpected difference in the

impedance responses of a nafion layer might be due to its different interference with S-LiOH and S-NaOH.<sup>36</sup>

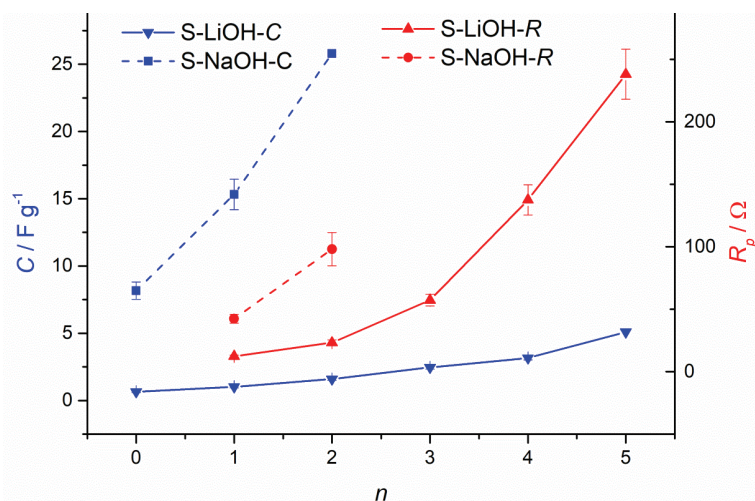


Fig. 4. The pore resistance ( $R_p$ ) and capacitance ( $C$ ) distribution throughout the porous structure of S-LiOH and S-NaOH. The values were obtained by fitting the data from Fig. 3 to 5- and 2-branched transmission line equivalent electrical circuits, respectively (the error bars, represent standard deviation of the fitting data).

Higher number of the branches required for the S-LiOH sample indicates its more complex structure, as a consequence of the smaller pore dimension of the S-LiOH in comparison to the S-NaOH (3.0 vs. 3.3 nm)<sup>27</sup> and higher micropores' volume (0.20 vs. 0.16 cm<sup>3</sup> g<sup>-1</sup>)<sup>27</sup>, causing its active sites harder to access. The overall capacitances calculated from the EIS results (Fig. 4) were 49.3 and 14.0 F g<sup>-1</sup> for S-NaOH and S-LiOH, respectively. These values correlate to the overall pore resistance throughout the branches, *i.e.*, 140 Ω for S-NaOH and 468 Ω for S-LiOH. It can be concluded that S-NaOH sample is of more accessible structure, hence its pore resistance was lower due to the wider pores and consequently its active sites were more accessible to the electrolyte giving higher capacitance values. This is in accordance to CV results, showing that S-NaOH sample is of higher CV currents, *i.e.*, the capacitance values calculated from CV response were higher for this samples too, compared to the S-LiOH.

#### CONCLUSION

The treatment with alkalis causes a multi-fold increase in the capacitance of carbonaceous materials synthesized by sucrose pyrolysis, but the stability of the capacitive features during continuous charging/discharging is intrinsic. The capacitance during charging/discharging cycles initially increases and afterwards



decreases. This feature is found to be caused by the continuous penetration of the electrolyte through the adhesion-ensuring nafion layer at the top of carbon layer.

The carbon layers activated with an alkali of small metal radius are of more developed porous structure, which is analyzed through the distributions of the capacitance and pore resistance, gained by impedance measurements. Although being of the more developed nanoporous structure, more compact layers are less available for charging/discharging processes and hence of modest capacitive characteristics.

The capacitive characteristics are more improved if the alkalis containing metal of the larger ionic radius are used for treatment. The correlation between capacitive features and physical characteristics of the carbon structure is suggested. The alkalis of larger radii of a metal are able to generate wider pores and consequently the structure of a porous layer more accessible for the charge transfer of capacitive response, which appears to be closely related to the degree of modification of the surface carbon particles.

#### SUPPLEMENTARY MATERIAL

Additional data and information are available electronically at the pages of journal website: <https://www.shd-pub.org.rs/index.php/JSCS/article/view/11960>, or from the corresponding author on request.

*Acknowledgement.* This work was funded by the Serbian Ministry of Education, Science and Technological Development Grant No. 451-03-68/2022-14/200026.

#### ИЗВОД

#### СУПЕРКАПАЦИТИВНА СВОЈСТВА УГЉЕНИЧНИХ МАТЕРИЈАЛА ДОБИЈЕНИХ ИЗ САХАРОЗЕ И АКТИВИРАНИХ ХИДРОКСИДИМА АЛКАЛНИХ МЕТАЛА

МИЛИЦА Г. КОШЕВИЋ<sup>1</sup>, САЊА С. КРСТИЋ<sup>2</sup>, ВЛАДИМИР В. ПАНИЋ<sup>1,3,4</sup> И БРАНИСЛАВ Ж. НИКОЛИЋ<sup>5</sup>

<sup>1</sup>Институт за хемију, технологију и металургију, Институт од националног значаја за републику Србију, Универзитет у Београду, Београд, <sup>2</sup>Институт за нуклеарне науке „Винча“, Универзитет у Београду, Београд, <sup>3</sup>Центар изузетних вредности, Институт за хемију, технологију и металургију, Институт од националног значаја за републику Србију, Универзитет у Београду, Београд, <sup>4</sup>Државни универзитет у Новом Пазару, Дејаршман за природно–математичке науке, Нови Пазар и <sup>5</sup>Технолошко–металуршки факултет, Универзитет у Београду, Београд

Испитиван је утицај различитих активирајућих хидроксида на електрохемијска својства активираних угљеничних материјала. Угљенични материјал је добијен хидротермалним третманом сахарозе, а потом активирањем помоћу КОН, NaOH и LiOH. Електрохемијска својства добијених узорака испитивана су цикличном волтаметријом и спектроскопијом електрохемијске импеданције. Синтетизовани материјали показују капацитивна својства. Највећа специфична капацитивност добијена је за узорак третиран помоћу КОН, док капацитивност прати величину пречника јона метала из алкалије којом је активирањем угљенични материјал.

(Примљено 30. јуна, ревидирано и прихваћено 18. јула 2022)

## REFERENCES

1. B. K. Saikia, S. M. Benoy, M. Bora, J. Tamuly, M. Pandey, D. Bhattachary, *Fuel* **282** (2020) 118796 (<https://doi.org/10.1016/j.fuel.2020.118796>)
2. A. González, E. Goikolea, J. A. Barrena, R. Mysyk, *Renew. Sustain. Energy Rev.* **58** (2016) 1189 (<https://doi.org/10.1016/j.rser.2015.12.249>)
3. Y. Liu, S.P. Jiang, Z. Shao, *Mater. Today Adv.* **7** (2020) 100072 (<https://doi.org/10.1016/j.mtadv.2020.100072>)
4. D. Sačer, M. Kralj, S. Sopčić, M. Košević, A. Dekanski, M. K. Roković, *J. Serb. Chem. Soc.* **82** (2017) 411 (<https://doi.org/10.2298/JSC170207027S>)
5. G. Šekularac, M. Košević, A. Dekanski, V. Djokić, M. Panjan, V. Panić, *ChemElectroChem* **4** (2017) 2535 (<https://doi.org/10.1002/celec.201700609>)
6. D. M. Mijailović, M. M. Vukčević, Z. M. Stević, A. M. Kalijadis, D. B. Stojanović, V. V. Panić, Petar S. Uskoković, *J. Electrochem. Soc.* **164** (2017) A1061 (<https://doi.org/10.1149/2.0581706jes>)
7. V. N. K. S. K. Nersu, B.R. Annepu, S. S. B. Patcha, S. S. Rajaputra, *J. Electrochem. Sci. Eng.* **12** (2022) 451 (<http://dx.doi.org/10.5599/jese.1310>)
8. A. S. Dobrota, I. A. Pašti, *J. Electrochem. Sci. Eng.* **10** (2020) 141 (<https://doi.org/10.5599/jese.742>)
9. D. M. Mijailović, V. V. Radmilović, U. Č. Lačnjevac, D. B. Stojanović, V. D. Jović, V. R. Radmilović, P. S. Uskoković, *Appl. Surf. Sci.* **534** (2020) 147678 (<https://doi.org/10.1016/j.apsusc.2020.147678>)
10. I. I. G. Inal, S. M. Holmes, A. Banford, Z. Aktas, *Appl. Surf. Sci.* **357** (2015) 696 (<https://doi.org/10.1016/j.apsusc.2015.09.067>)
11. G. Dhakal, D. Mohapatra, Y-II Kim, J. Lee, W. K. Kim, J-J. Shim, *Renew. Energy* **189** (2022) 587 (<https://doi.org/10.1016/j.renene.2022.01.105>)
12. Y. Zhu, Z. Li, Y. Tao, J. Zhou, H. Zhang, *J. Energy Storage* **47** (2022) 103624 (<https://doi.org/10.1016/j.est.2021.103624>)
13. Y. Chen, Y. Yu, X. Zhang, C. Guo, C. Chen, S. Wang, D. Min, *Ind. Crops Prod.* **181** (2022) 114802 (<https://doi.org/10.1016/j.indcrop.2022.114802>)
14. S. J. Rajasekaran, V. Raghavan, *J. Electrochem. Sci. Eng.* **12** (2022) 545 (<http://dx.doi.org/10.5599/jese.1314>)
15. G. Radić, I. Šajnović, Ž. Petrović, M.K. Roković, *Croat. Chem. Acta* **91** (2018) 481 (<https://doi.org/10.5562/cca3452>)
16. D. Sačer, I. Spajić, M. K. Roković, *J. Mater. Sci* **53** (2018) 15285 (<https://doi.org/10.1007/s10853-018-2693-6>)
17. S. S. Rajaputra, N. Pennada, A. Yerramilli, N. M. Kummara, *J. Electrochem. Sci. Eng.* **11** (2021) 197 (<https://doi.org/10.5599/jese.1031>)
18. M. Xu, A. Wang, Y. Xiang, J. Niu, *J. Clean. Prod.* **315** (2021) 128110 (<https://doi.org/10.1016/j.jclepro.2021.128110>)
19. S. Sopčić, N. Šešelj, M. K. Roković, *J. Solid State Electrochem.* **23** (2019) 205 (<https://doi.org/10.1007/s10008-018-4122-9>)
20. H. Pan, J. Li, Y. Feng, *Nanoscale Res. Lett.* **5** (2010) 654 (<https://doi.org/10.1007/s11671-009-9508-2>)
21. M. Karnan, A. G. Karthick Raj, K. Subramani, S. Santhoshkumara, M. Sathish, *Sustain. Energy Fuels* **4** (2020) 3029 (<https://doi.org/10.1039/C9SE01298B>)
22. S. Ahmed, A. Ahmed, M. Rafat, *J. Saudi Chem. Soc.* **22** (2018) 993 (<https://doi.org/10.1016/j.jscs.2018.03.002>)

23. X. Cai, Y. Xiao, W. Sun, F. Yang, *Electrochim. Acta* **406** (2022) 139861 (<https://doi.org/10.1016/j.electacta.2022.139861>)
24. S. Pang, L. Lin, Y. Shen, S. Chen, W. Chen, N. Tan, A. Ahmad, A. A. Al-Kahtani, A. M. Tighezza, *Mater. Lett.* **315** (2022) 131985 (<https://doi.org/10.1016/j.matlet.2022.131985>)
25. J. Xu, L. Chen, H. Qu, Y. Jiao, J. Xie, G. Xing, *Appl. Surf. Sci.* **320** (2014) 674 (<https://doi.org/10.1016/j.apsusc.2014.08.178>)
26. X. H. P. Ling, M. Yu, X. Wang, X. Zhang, M. Zheng, *Electrochim. Acta* **105** (2013) 635 (<https://doi.org/10.1016/j.electacta.2013.05.050>)
27. S. S. Krstić, M. M. Kragović, V. M. Dodevski, A. D. Marinković, B. V. Kaluđerović, G. Žerjav, A. Pintar, M. C. Pagnacco, M. D. Stojmenović, *Sci. Sinter.* **50** (2018) 255 (<https://doi.org/10.2298/SOS1802255K>)
28. B. Zdravkov, J. Čermák, M. Sefara, Josef Janků, *CEJC* **5** (2007) 385 (<https://doi.org/10.2478/s11532-007-0017-9>)
29. E. Frackowiak, *Phys. Chem. Chem. Phys.* **9** (2007) 1774 (<https://doi.org/10.1039/B618139M>)
30. M. Quan, D. Sanchez, M. F. Wasylkiw, D. K. Smith, *J. Am. Chem. Soc.* **129** (2007) 12847 (<https://doi.org/10.1021/ja0743083>)
31. O. Gharbi, M. T. T. Tran, B. Tribollet, M. Turmine, V. Vivier, *Electrochim. Acta* **343** (2020) 136109 (<https://doi.org/10.1016/j.electacta.2020.136109>)
32. M. R. Pantović Pavlović, M. M. Pavlović, S. Eraković, J. S. Stevanović, V. V. Panić, N. Ignjatović, *Mater. Lett.* **261** (2020) 127121 (<https://doi.org/10.1016/j.matlet.2019.127121>)
33. S. Kaiser, M. S. Kaiser, *J. Electrochem. Sci. Eng.* **10** (2020) 373 (<https://doi.org/10.5599/jese.877>)
34. L. Miao, Z. Song, D. Zhu, L. Li, L. Gan, M. Liu, *Mater. Adv.* **1** (2020) 945 (<https://doi.org/10.1039/D0MA00384K>)
35. H. L. K. S. Mosch, O. Akintola, W. Plass, S. Hoepfner, U. S. Schubert, A. Ignaszak, *Langmuir* **32** (2016) 4440 (<https://doi.org/10.1021/acs.langmuir.6b00523>)
36. V. V. Panić, A. B. Dekanski, V. B. Mišković-Stanković, B. Ž. Nikolić, *Chem. Biochem. Eng. Q.* **23** (2009) 23.